

Energy-efficient path planning for fully propelled AUVs in congested coastal waters

Teong-Beng Koay and Mandar Chitre

Acoustic Research Laboratory, Tropical Marine Science Institute

National University of Singapore, Singapore 119227

{koay, mandar}@arl.nus.edu.sg

Abstract—To navigate safely in littoral waters with complex currents and busy shipping activities, it is crucial to have small autonomous vehicle with full propulsion capability. Such systems typically have limited endurance. We therefore investigate the feasibility of improving their endurance using current-aware path planning algorithms that allow active propulsion to move the vehicle into favorable currents or to avoid obstacles. The strategy adopted is to minimize the use of propulsion while leveraging favorable currents as much as possible. We perform simulations using environmental data and operational constraints of autonomous vehicles. The current field is assumed to be time-invariant over the period of the mission. Simulation results for 40 randomly generated source-destination pairs in Singapore Strait are presented. The performance is quantified by comparing the energy consumption of the path generated against the shortest distance path. Simulation results show that we are able to save 30–90% energy if the vehicles are allowed to drift along with the current. When the minimum speed of the vehicle is constrained to 2.5 knots, the energy savings could range from a few percent to more than 50%, depending on the currents along the route. The expected energy saving is the largest when the vehicle is allowed to operate at speeds comparable to water current while the savings diminish when the vehicle is required to operate at higher speed.

I. INTRODUCTION

Modern autonomous vehicles play an increasing role in environmental monitoring and exploration with the expectation of reduced logistics and operational cost. Nevertheless, their usefulness is limited by their operational endurance. This translates to a limited range that they can effectively cover.

To navigate an autonomous vehicle efficiently under the influence of spatially inhomogeneous currents is a challenging task. This is especially true in littoral-coastal environments where complex bathymetry, islands and fresh water outlets intensify the complexity of the current field. Apart from the challenges of obstacle avoidance, the large energy consumption needed to navigate these environments significantly limits the range of a typical Autonomous Underwater Vehicles (AUVs).

A number of researches have looked into improving the vehicle endurance by extending the energy capacity [1]–[3] and moving away from power hungry propulsion technology [4]–[6]. Majority of these systems are very sensitive to water current. Hence, significant research has been invested into effective path planning using ocean models [7]–[10].

In recent years, current-aware energy efficient path planning has been partially studied. Approaches such as level set

method [11], genetic algorithms [12], time minimization using search algorithms [13], [14], particle swarm optimization [15], and Lagrangian coherent structures [16] can be found in simulation studies. Recent literature shows that it is feasible to steer a drifter between waypoints in a broad sense or to stay within a region using appropriate current variations [17]–[19].

To date, a handful of experimental studies on the current-aware path planning have been carried out in relatively open water [15], [20]. However, operation of these technologies is significantly impeded by the strong currents, busy shipping channels, complex geographical structures and limited water depth. Notably, the risk of collision and the associated economic cost is high in port regions such as Shanghai, Singapore, Rotterdam, Busan and many others.

The complexity of operating in such a region is clearly shown by Figure 1. For instance, Singapore has more than 60 islands intertwined with numerous shipping lanes used by some 120,000 large commercial vessels visiting her each year [21]. There are about 800 vessels distributed in these waters at any one time [22], while the effective traffic density is higher when smaller support vessels and recreational craft are taken into account. Additionally, the surrounding waters contain complex regional hydrodynamics due to the dense islands and complicated bathymetry.



Fig. 1: Challenges in congested coastal waters: Cluttered islands, busy shipping activities, and complex water currents. This is a satellite picture showing a section of coastal waters in Singapore Strait, source: Google Maps.

These conditions have made the operations of small low power platforms such as Lagrangian drifters and glider-like

vehicles difficult and undesirable. Other large-size, long-range vehicles would also find it difficult to operate here due to space and logistic constraints.

We argue that it would take a fully propelled vehicle to mitigate the risk of collisions and navigate safely within these waters. With the exception of specialized long-range vehicle such as Tethys [23], typical small general-purpose vehicles are limited in endurance. The objective of this study is to extend the endurance of small fully propelled AUVs without having to rely on carefully designed drag-efficient form-factor. We therefore explore potential algorithms that allow these vehicles to minimize propulsion by taking advantage of local current to assist them in reaching desired waypoints.

We described the challenges of operating AUVs within congested coastal water in this section. We then present the problem statement and formulation of the approach in Section II. This is followed by the description of simulation setup in Section III, the different heuristics in Section IV, and their performances in Section V. Lastly, we conclude and describe the ongoing work in Section VI.

II. ENERGY EFFICIENT PATH PLANNING

We wish to find a path for an AUV to navigate in the presence of currents and obstacles while consuming minimum amount of propulsion energy. Additionally, we allow the vehicle to increase its propulsion to counter the current and avoid collisions when necessary.

Let $Q \subset \mathbb{R}^2$ be a 2-dimensional search space, with $L \subset Q$ be the landmass. $P = Q - L$, is a potentially concave search space representing the water an AUV operates in. We assume that the currents $c(p)$, $p \in P$, are known and do not change over the course of the AUV mission. This can be extended to time varying fields in the future by adding a time variable.

The objective is to plan a path between any two points $n_i, n_j \in P$ in such a way that the AUV takes advantage of the currents in the operational area and minimizes the amount of energy used. Assuming the hotel load¹ and energy consumption of sensor payloads in the vehicle are much smaller than the energy its propulsion system requires, we only consider the energy needed to propel the AUV through water in the cost function. The efficiency of the propulsion system adds another term that increases the energy consumption as a function of thrust speed. For simplicity, we assume that the efficiency of the propulsion system is constant.

The energy needed to propel the vehicle is related to the work to overcome the drag induced by relative current as the vehicle moves through water. This relative current is quantified by the vehicle's thrust speed v_t , and can be estimated as follows. Let $v_g, v_t \in \mathbb{R}^2$ be the vehicle's thrust velocity, and ground velocity respectively with the following relationship:

$$v_g = c + v_t. \quad (1)$$

To reach the next waypoint, we align v_g along the direction from n_i to n_j . Hence, v_g has the direction $\theta = \angle(n_j - n_i)$.

¹Power consumption of base vehicle excluding the propulsion.

We also keep the ground speed v_g , as a variable in order to minimize v_t so that the propulsion is minimized. We then obtain the optimum v_g by minimizing v_t :

$$v_g^* = \arg \min_{v_g} \left| v_g \begin{pmatrix} \cos \theta \\ \sin \theta \end{pmatrix} - c \right|, v_g > 0. \quad (2)$$

The ground speed v_g should be larger than 0 for the vehicle to move towards its waypoint. When the AUV is required to reach n_j within a certain time constraint, v_g has an increased lower bound, which in turn increases the energy consumption. This time constrained path planning is not included in the scope of this paper.

The optimum thrust velocity is then obtained by:

$$v_t^* = v_g^* \begin{pmatrix} \cos \theta \\ \sin \theta \end{pmatrix} - c. \quad (3)$$

We limit the AUV's thrust speed within desired upper and lower limits based on limitation of propulsion system and requirement from path planning heuristics. Let the speed limits be $k = (k_{\min}^{k_{\max}})$, the thrust speed is then given by:

$$v_t = \begin{cases} k_{\max} \frac{v_t^*}{|v_t^*|} & \text{if } |v_t^*| > k_{\max}, \\ k_{\min} \frac{v_t^*}{|v_t^*|} & \text{if } |v_t^*| < k_{\min}, \\ v_t^* & \text{otherwise.} \end{cases} \quad (4)$$

With v_t and v_g obtained, the energy needed to travel n_i to n_j can be calculated from the product of vehicle speed through water, drag force it experiences, and the travel duration. By keeping distance between n_i and n_j shorter than the current scale, the current between them can be assumed homogeneous. Hence, the energy term can be written as:

$$\begin{aligned} E(n_i, n_j, c, k) &= v_t \times v_t^2 K \times \frac{|n_i - n_j|}{v_g} \\ &= v_t^3 K \frac{|n_i - n_j|}{v_g}, \end{aligned} \quad (5)$$

where,

K = Drag constant based on the vehicle design,

v_t, v_g = Vehicle relative and ground speeds obtained from (2)–(4) based on n_i, n_j, c , and k .

Note that the amount of energy to overcome the drag is proportional to the cube of v_t , but only inversely proportional to ground speed v_g . Therefore, it is desirable to keep the thrust speed as low as possible, even with the cost of slower ground speed. Nevertheless, in actual operation, this is limited by:

- 1) Upper and lower bounds of the thrust power a vehicle can produce.
- 2) The time constraint for the vehicle to reach the destination.

An A* search [24] framework is then used to find the path that minimizes the total amount of energy needed to overcome the drag along the entire path. Let the starting and destination points be $s, d \in P$, an intermediate waypoint be n_i , and B be an ordered set of waypoints $\{b_0, b_1, \dots, b_{j-1}, b_j\}$, $j \in \mathbb{N}^+$.

The cost function used in the search for the best path from s to d through n_i is given by:

$$f(s, n_i, d, c, k) = g(B_i, c, k) + h(n_i, d, c, k), \quad (6)$$

where B_i is a path from $b_0 = s$ to $b_j = n_i$.

The term $g(B_i, c, k)$ is the energy cost to travel from s to n_i along the best known path B_i at any point of the search process. Note that B_i may evolve during the search process. The second term $h(n_i, d, c, k)$ is the predicted energy cost to travel from n_i to d using heuristics to be described in Section IV.

The best known energy cost to reach n_i can be obtained by aggregating the work done to travel between the waypoints. Employing (5), the energy cost can be written as:

$$g(B_i, c, k) = \sum_{k=1}^j E\left(b_{k-1}, b_k, c\left(\frac{b_{k-1} + b_k}{2}\right), k\right). \quad (7)$$

Function $h(\cdot)$ estimates the cost to travel from n_i to d using heuristic $H(\cdot)$. Here, $H(\cdot)$ abstracts the current condition along the journey into a representative current \tilde{c} , which $h(\cdot)$ uses to estimate the energy needed as the following:

$$h(n_i, d, c, k) = E(n_i, d, \tilde{c}, k). \quad (8)$$

For this purpose, v_g is aligned along n_i to d , i.e., $\theta = \angle(d - n_i)$, while calculating (2)–(5).

As the search progresses and eventually reaches d , we obtain the current-aware energy efficient path:

$$B_d = \{b_0, b_1, \dots, b_{j-1}, b_j\}, \text{ where } b_0 = s, b_j = d. \quad (9)$$

The total energy required to travel the path is:

$$W = \sum_{k=1}^j E\left(b_{k-1}, b_k, c\left(\frac{b_{k-1} + b_k}{2}\right), k\right). \quad (10)$$

III. SIMULATION SETUP

The simulation studies use operational parameters that are as close as possible to the real AUV operations. They include the speed constraints k and drag coefficient K that are based on physical design from STARFISH AUVs [25], as well as the current model [26] for Singapore Strait. The simulations also take into account geographical locations of landmasses. The search is performed on the same 2-dimensional grid used by the hydrodynamic forecast system. Shipping traffic and any errors in the current prediction are ignored in this paper.

A. The hydrodynamic model used in simulation

The current information within the operation region is taken from an ocean current hydrodynamic forecast model called Tropical Marine Hydrodynamics (TMH) [27]–[29]. It is a data driven hydrodynamic model that takes into account local bathymetry, tidal currents, monsoon effects, and boundary condition based on larger regional model. These hydrodynamic forecasts can be obtained from Live Access Server (LAS) [26]. A sample of the water current forecast is shown in Figure 2. It shows that the local water current contains significant spatial

variations that can potentially be exploited, depending on the positions of the source and destination points.

The TMH model provides forecast of temporally averaged current in the region in half hourly time slots starting from the midnight of each day. The current vectors are assumed to be temporally static within the time slot. The spatial current information is provided with grid the size of approximately 76m by 65m. The current prediction for the water column is divided into 3 layers. Only the top layer is used in this paper.

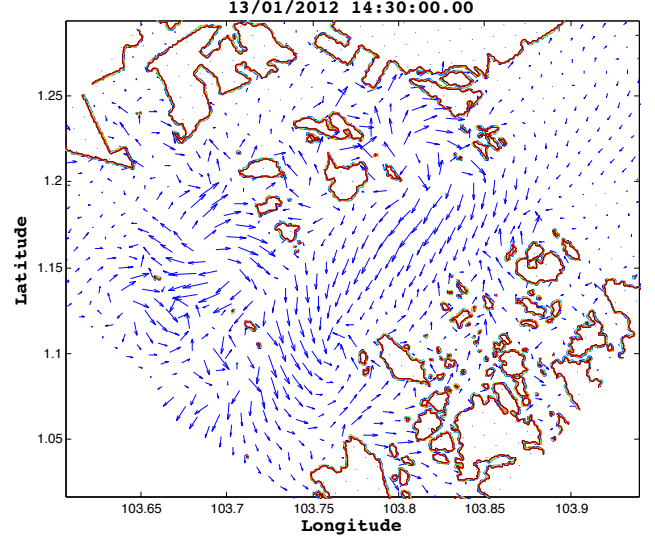


Fig. 2: Typical current field in the local water obtained from TMH hydrodynamic model.

B. The source-destination pairs used

All the source-destination pairs used in the simulation are points generated by a pseudo-random process. A set of points are first randomly generated, but only those located in the water with distances that are more than 15 km are accepted. This process is repeated until 40 source-destination pairs are obtained. This resulted in source-destination pairs with distance ranges from about 17 km to 34 km. More than 80% of these location pairs have landmass in between them with different degree of obstructions (Figure 3).

C. The benchmark route

The benchmark path is generated by the same A* search framework described in Section II, using only distance as the cost function:

$$f(s, n_i, d) = g(B_i) + h(n_i, d), \quad (11)$$

$$g(B_i) = \sum_{k=1}^j |b_k - b_{k-1}|, \quad (12)$$

$$h(n_i, d) = |d - n_i|. \quad (13)$$

This generates a shortest distance path from s to d at the end of the search. The benchmark energy consumption for each of the source-destination pairs is then calculated by evaluating

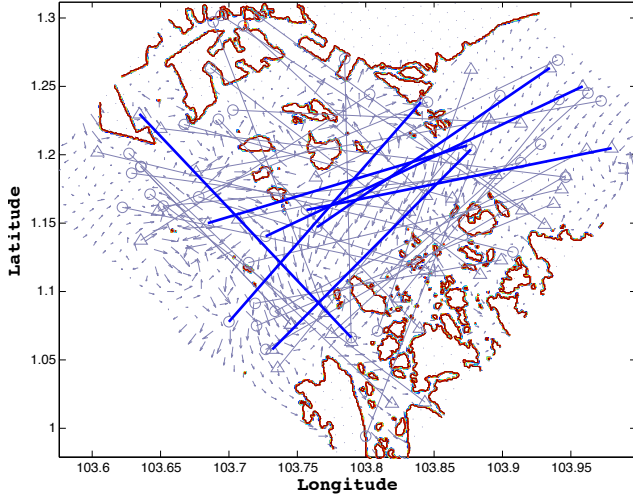


Fig. 3: Randomly generated source-destination pairs used in simulation. Only a small number of them (thick lines) have no obstacle in between start and end points.

their respective benchmark paths using (10). As part of the $E(\cdot)$ calculation using (1) to (5), the propulsion along the benchmark path is set at the lowest possible level needed to maintain desired bearing or k_{\min} , whichever is higher.

With this approach, we maintain the same simulation criteria as that used in evaluating different algorithms. Each source-destination pairs is evaluated in both directions to minimize any potential bias in the statistics of the result due to geographical advantage. This approach is able to find the shortest path through islands as shown in Figure 4.

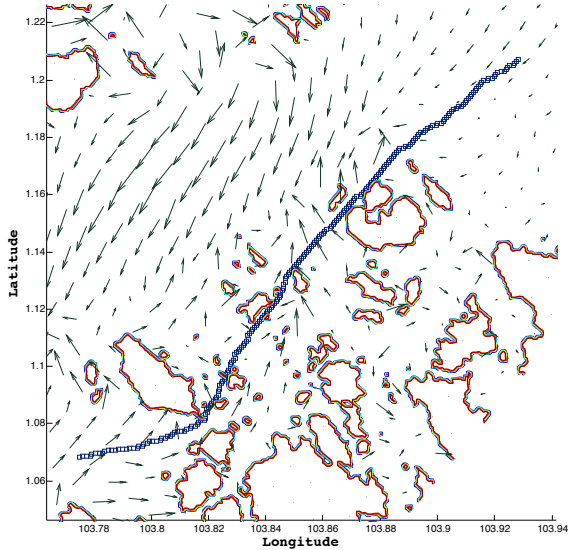


Fig. 4: An example of the benchmark path planned through a group of islands, ignoring the effects of water currents.

IV. THE HEURISTICS

The quality of the search largely depends on the heuristics that guide the search to minimize any unnecessary explorations. A *consistent heuristic*² would be the most efficient, but this is not guaranteed in the search for current-aware path due to the spatially varying currents that exist in the search space. For this, we employ heuristics that are *admissible*³ to ensure the search return an optimum result.

The heuristic $H(\cdot)$ first finds the shortest distance path between n_i and d in a similar way to Section III-C. This provides a list of ordered waypoints in the coastal waters that are spaced shorter than the scale of the currents:

$$B'_i = \{b_0, b_1, \dots, b_{j-1}, b_j\}, \quad b_0 = n_i, \quad b_j = d.$$

The heuristic also modifies the limits of the vehicle thrust speeds k as needed. It then estimates an equivalent current \tilde{c} that captures the spatial variations of the currents along the waypoints. The heuristic cost function $h(\cdot)$ then employs (2)–(5) using \tilde{c} and k to estimate v_t , v_g , and lastly the energy needed to reach d . Some of the promising heuristics used for $H(\cdot)$ are presented in this section.

A. Largest favorable current

This heuristic $H(\cdot)$ looks for the largest current at any point along B'_i that loosely flows towards the destination.

Algorithm 1 Largest favorable current.

Require: n_i, d, c

$B'_i \leftarrow$ Shortest path waypoints from n_i to d

Set $\tilde{c} \leftarrow \min(c)$

for all $n \in B'_i$ **do**

if $|c(n)| > |\tilde{c}|$ **and** $|\angle c(n) - \angle v_t| < 90^\circ$ **then**

$\tilde{c} \leftarrow c(n)$

end if

end for

$k_{\min} \leftarrow$ AUV cruising speed

return \tilde{c}, k_{\min}

In this case, $h(\cdot)$ causes the search to favor the directions that contain larger favorable current towards the destination. Excluding the currents not in the same general directions towards d ensures that the heuristics will not over estimate the cost to reach d . Hence, it makes the algorithm admissible. A potential limitation of this approach is that it reduces to shortest-path search if no favorable current exist in the search space.

B. Best net current

In this approach, $H(\cdot)$ uses the sum of all the current vectors along B'_i as a summary of the current field. The currents in the favorable directions are given a higher weighting, where the

²A heuristic that estimates the cost such that search progress towards destination without stepping back.

³ $h(n_i, d, c) \leq C(n_i, d, c), \forall n_i$, where $C(n_i, d, c)$ is the actual cost to travel from n_i to d .

weighting factor $w_h \in \mathbb{R}^+$, is increased to $w > 1$, when the direction of the current $c(n)$ is in the same general direction as the bearing towards the destination. In this paper, w is simply 2. $H(\cdot)$ is given as the following:

Algorithm 2 Best net current.

Require: n_i, d, c

$B'_i \leftarrow$ Shortest path waypoints from n_i to d

Set $\tilde{c} \leftarrow 0$

Set $j \leftarrow 0$

for all $n \in B'_i$ **do**

$j \leftarrow j + 1$

if $|\angle c(n) - \angle v_t| < 90^\circ$ **then**

Set $w_h \leftarrow w$

else

Set $w_h \leftarrow 1$

end if

$\tilde{c} \leftarrow \tilde{c} + w_h c(n)$

end for

$\tilde{c} \leftarrow \tilde{c} / j$

$k_{\min} \leftarrow$ AUV cruising speed

return \tilde{c}, k_{\min}

This approach is intended to overcome the shortcoming of the heuristic in Section IV-A, which does not make active decisions when all currents in the field are unfavorable to the desired path. By making decisions based on the net current, a direction is always be rewarded or penalized. This gives continuity in the heuristic assessment.

C. Small currents

This method searches for the route with the least amount of current along B'_i , irrespective of its direction. $H(\cdot)$ is given by:

Algorithm 3 Small currents.

Require: n_i, d, c

$B'_i \leftarrow$ Shortest path waypoints from n_i to d

Set $\tilde{c} \leftarrow \max(c)$

for all $n \in B'_i$ **do**

if $|c(n)| < |\tilde{c}|$ **then**

$\tilde{c} \leftarrow c(n)$

end if

end for

$k_{\min} \leftarrow$ AUV cruising speed

return \tilde{c}, k_{\min}

This heuristic considers only the smallest currents and ignores the larger currents that could exist at some sections along B'_i . This allows the search to work better when small patches of large currents co-exist in an area with mainly slow current.

D. Drift with favorable currents

This is a special case of the heuristic described in Section IV-A, where the lower limit of the vehicle thrust is

lowered to ensure that the vehicle is able to drift with current. It looks for the maximum favorable current and only thrusts as much as needed get to get into the favorable currents. The same heuristic as the one in section IV-A is used, except that the lower thrust limit is set to be smaller than the known current in the field,

$$k_{\min} < \min(|c|).$$

Figure 5 shows that the path generated using this heuristic takes better advantage of the currents than others. Hence, it saves the largest amount of energy among the heuristics tested. The disadvantage of this strategy is that the effective ground speed of the path largely depends on the velocity of the favorable currents. In this particular simulation scenario, the travel time needed is much longer as compared to other heuristics because most of the path has small current and the vehicle has taken a long detour.

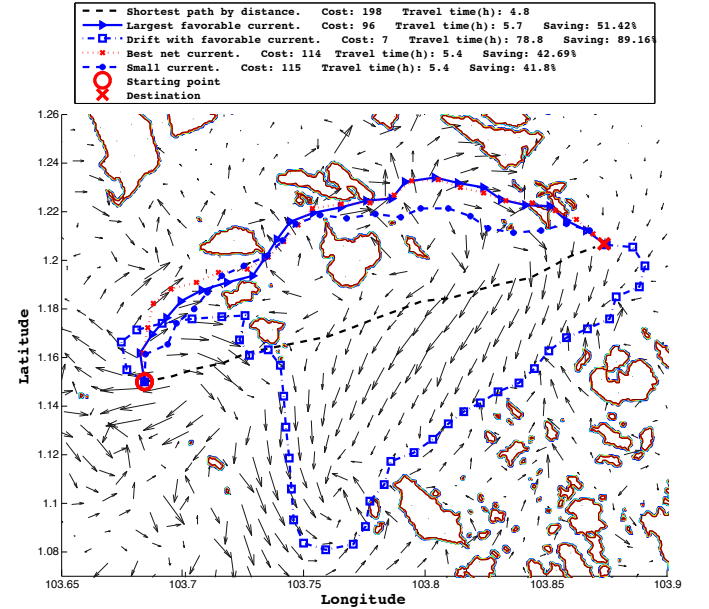


Fig. 5: A route that drifts along with the favorable currents.

Typically, most AUVs need a minimum thrust to dive. This means that most AUVs using this heuristic would have to operate on the surface unless they are able to actively control their buoyancy. Although the travel duration of the generated path could be long, this method could contribute to operations where surface expressions and operational speed are not constraints, as in Lagrangian buoy's operations [16] [30]. The advantage of this approach is its capability to generate feasible routes with occasional propulsion. Therefore, its ability to generate feasible paths is not solely at the mercy of the regional current variations as Lagrangian buoys [18].

V. RESULTS

Apart from the heuristic that allows the AUV to drift with current, all other heuristics allow the AUV to thrust between 2.5–5 knots through the water. These numbers are

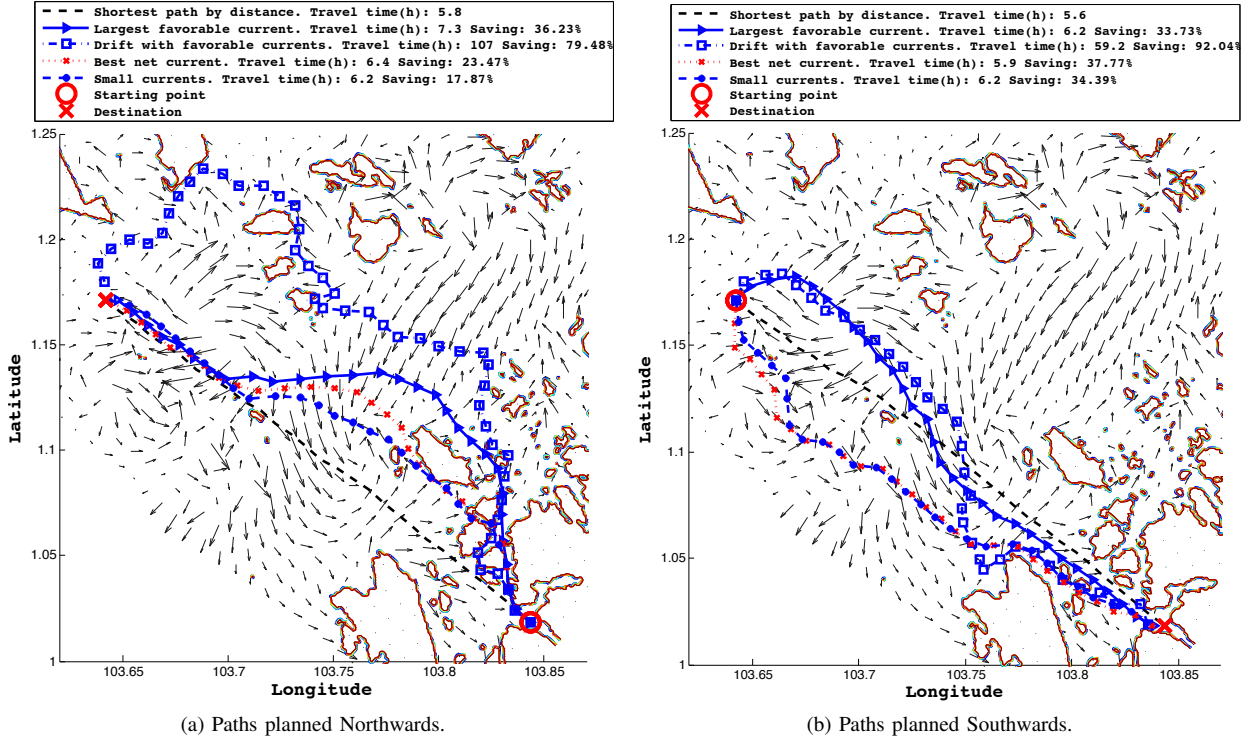


Fig. 6: The paths generated by different heuristics on same pair of locations. Left and right figures show the different paths generated when the starting and end points are swapped.

selected based on the cruising speed and upper speed limit of STARFISH AUVs. This prepares the simulation results for comparison with results from upcoming experiments.

A. Overall performance

Figure 6 shows the paths generated for a source-destination pair using different heuristics while keeping other operating criteria the same. The heuristics are able to lock on to the favorable currents effectively. The heuristic from Section IV-D provides the largest energy saving (over 75%), but it also significantly increases travel time. When the currents are not in favor of traveling along the direct path, the heuristics are able to make detours with the help of some propulsion and take advantage of the current. This is noticeable when the vehicle is required to move northwards, where almost half of the journey experiences unfavorable currents. The algorithms are able to generate routes that take advantage of the sheltered regions among the islands and get into favorable positions that avoid head-on currents. The heuristics described in IV-B and IV-C perform modestly compared to the first two heuristics, but they are expected to work well when the currents in the fields are not in favor of the direction of travel.

Subsequently, 40 source-destination pairs are simulated employing the heuristics described in the previous section, each evaluated along both directions. The results are tabulated into two histograms. The first histogram (Figure 7) shows the results when the vehicle's minimum thrust speed is set to

2.5 knots, and the second (Figure 8) shows the results when the vehicle is allowed to drift.

When the minimum speed is limited to 2.5 knots, the average energy saving is about 23% with a maximum of about 48%. About 2.5% of the routes perform a little worse (spent up to 4% more energy) compared to the benchmark path. The paths typically require an average of 6% extra time to travel compared to their benchmark paths. In the presence of some difficult currents, up to 35% extra time is needed. While under some good currents, we save a few percent of the travel time.

When the vehicle is allowed to drift, the scale of energy savings is also increased. Simulation shows energy savings range from about 30% to more than 90% with an average of about 73% (Figure 8); except one route that spends about 4% more energy than the benchmark path. Note that we currently do not take into account the hotel load, which would cap the maximum energy saving to a lower level.

B. The effects of thrust levels

The simulation results in the previous section show that the amount of energy savings is significantly affected by the AUV's minimum speed. In this section, we vary the lower limit of the thrust to investigate how it affects the energy saving. In this simulation setup, a single heuristic is used, and all other simulation criteria are kept the same with the exception of thrust.

Figure 9 shows the variations of energy savings at different

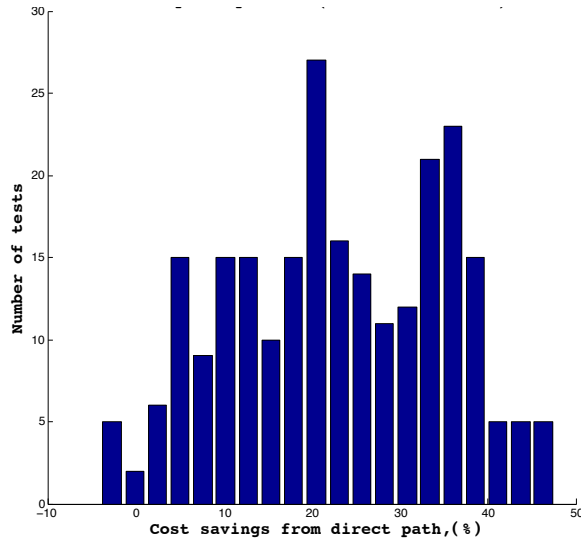


Fig. 7: Energy savings of current-aware paths compared to benchmark paths. Minimum thrust speed is limited to 2.5 knots in all cases.

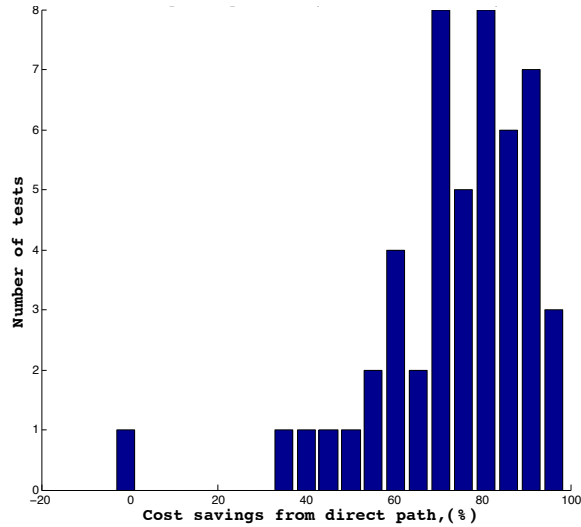


Fig. 8: Energy savings of current-aware paths compared to the shortest paths. Both are limited to minimum thrust of 0.2 knots.

thrusters. Note that the horizontal axis denotes the ratio of the lower bound of AUV speed to the mean of water speed along the planned path. It represents the ability of the vehicle to drift with the current if it chooses to, but not the absolute speed.

In general, the amount of energy savings increases as the lower bound of propulsion is reduced. When the vehicle is required to run at higher speeds than water currents, the advantage given by the currents tends to be smaller. This causes the distance of travel to be the dominant factor that determines the cost. Therefore, the energy consumption approximates the cost of shortest distance path algorithm as the vehicle speed increases. The simulation shows that the energy savings can

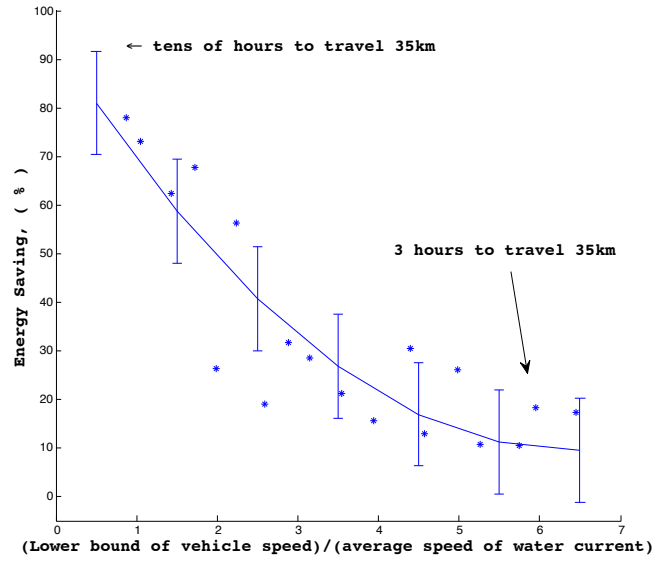


Fig. 9: Effects of lower bound of vehicle speeds to the energy savings. The solid line is a quadratic polynomial fit with standard error indicated by error bars. At the region with high energy savings, the actual travel time can be large as the effective ground speed become as small as the current speed.

be more than $70 \pm 10\%$ when the lower bound of vehicle speed is similar to water current.

Figure 10 shows the extra time spent against the energy savings when traveling a few of the simulated paths. For a 35 km route with a mean current of $0.35 \pm 0.1 \text{ ms}^{-1}$, the travel time needed ranges from a few to nearly 70% depending on the thrusts, and the availability of favorable currents. This translates to about 3 to more than 10 hours of extra travel time in the simulated paths. The simulation shows that allowing about 10–20% of extra traveling time finds routes that save 50% of energy or more.

Note that time of travel varies significantly as the energy savings approach 60% and above. This is because the propulsion is typically kept at its minimum in these scenarios, and the vehicle starts to rely on the current vectors to reach the destination. Therefore, the time of arrival tends to depend on the current's speed and direction. At places where the currents in the field are least favorable, the algorithm would need to find detours with favorable currents to the destination. This inevitably increases travel time; see paths with 0.25 and 0.5 ms^{-1} thrust speeds in Figure 11. When the currents are more favorable, savings in terms of travel time can be achieved (see Figure 10).

Figure 11 shows that many of the paths generated with higher minimum thrust travel in similar routes until a bifurcation occurred when the thrust is lowered to 0.5 ms^{-1} and below. The current-aware paths improve the energy savings across different thrust settings in this simulation. The results suggest that the lower bound of the thrust should be kept small, and only adjusted to control the time of arrival or to maintain controllability.

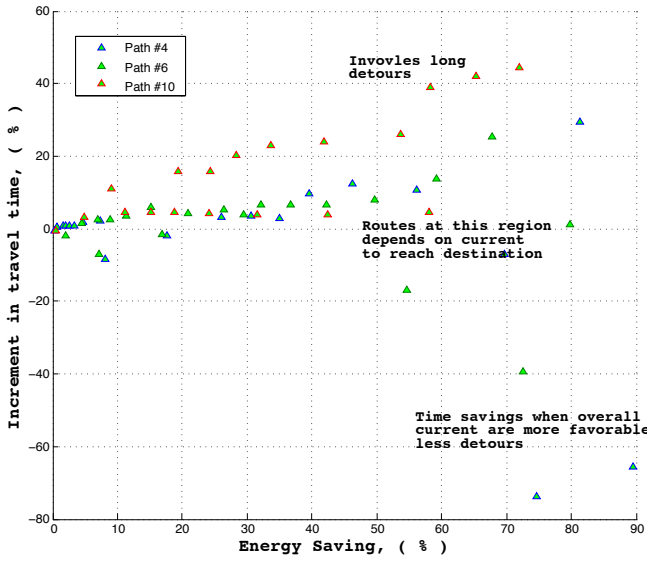


Fig. 10: Relationship of variations in travel time and energy savings. It can be seen that the variations of travel time increase as the energy saving increase. It seems that there are evidence of bifurcation around the 50–60% mark of energy savings that the variations of time travel increases drastically.

VI. CONCLUSIONS AND ONGOING WORKS

We argued that it takes a vehicle with capable propulsion system to operate safely in congested coastal waters. Such systems are typically power hungry; we proposed and investigated the feasibility to extend their endurance by planning current-aware energy-efficient paths in these waters.

A few basic heuristics were simulated, and the results showed that the slower the vehicle is allowed to travel, the more energy it can save at the cost of increased travel time.

The simulations showed that energy savings can reach around 50% if the lower bound of speed is set to 2.5 knots, depending on how favorable the currents in the field are. The traveling time of these routes are typically increased by 10–20% in the test scenarios. When the vehicle is allowed to drift, the current-aware paths are able to save up to 90% of propulsion energy.

We next plan to refine the heuristics to extend the studies to temporally varying fields. We also plan to include a reactive path planning algorithm to tackle the errors in the ocean current model based on the actual current observed in the field. A field experiment is also planned to test the current-aware path planning.

ACKNOWLEDGMENT

The authors would like to thank Dr Pavel Tkach and Mr Xu Haihua for making the TMH model available for this research.

REFERENCES

[1] P. Rynne and K. von Ellenrieder, "Development and preliminary experimental validation of a wind- and solar-powered autonomous surface vehicle," *Oceanic Engineering, IEEE Journal of*, vol. 35, pp. 971–983, October 2010.

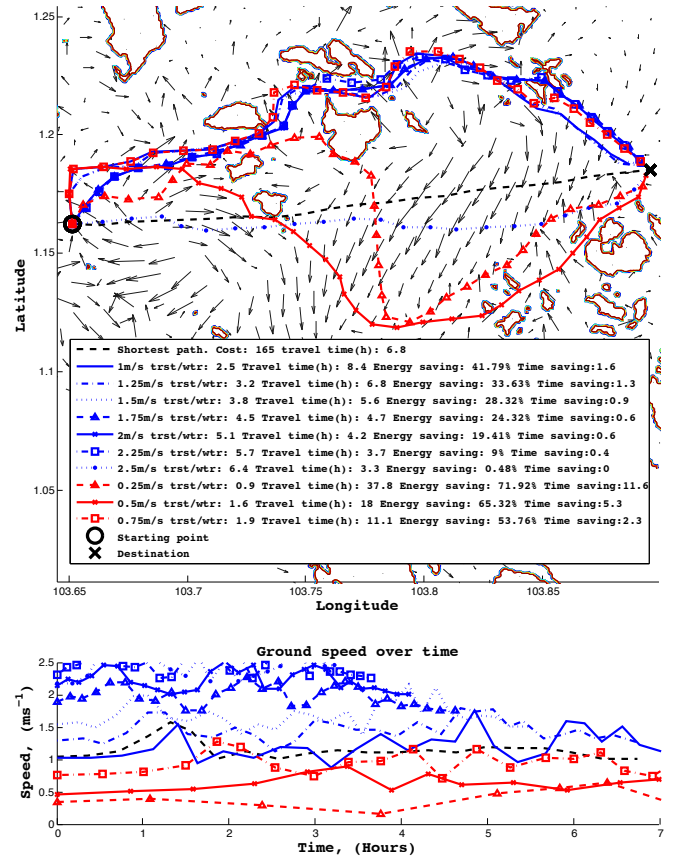


Fig. 11: Effects of thrust levels to the generated current-aware paths. Note that the ground velocities vary along the path as the algorithm changes the vehicle speed to counter stronger currents and maintain above the lower limit of thrust speed.

[2] D. Crimmins, C. Patty, M. Beliard, J. Baker, J. Jalbert, R. Komerska, S. Chappell, and R. Blidberg, "Long-endurance test results of the solar-powered AUV system," in *OCEANS 2006*, pp. 1–5, September 2006.

[3] M. Arima, T. Okashima, and T. Yamada, "Development of a solar-powered underwater glider," in *Underwater Technology (UT), 2011 IEEE Symposium on and 2011 Workshop on Scientific Use of Submarine Cables and Related Technologies (SSC)*, pp. 1–5, April 2011.

[4] J. Jaffe and C. Schurgers, "Sensor networks of freely drifting autonomous underwater explorers," in *Proceedings of the 1st ACM international workshop on Underwater networks, WUWNet '06*, (New York, NY, USA), pp. 93–96, ACM, 2006.

[5] J. Manley and S. Willcox, "The wave glider: A persistent platform for ocean science," in *OCEANS 2010 IEEE - Sydney*, pp. 1–5, may 2010.

[6] D. Webb, P. Simonetti, and C. Jones, "Slocum: an underwater glider propelled by environmental energy," *Oceanic Engineering, IEEE Journal of*, vol. 26, pp. 447–452, oct 2001.

[7] E. Fernández-Perdomo, J. Cabrera-Gómez, D. Hernández-Sosa, J. Isern-González, A. Domínguez-Brito, A. Redondo, J. Coca, A. Ramos, E. Fanjul, and M. García, "Path planning for gliders using regional ocean models: Application of pinzon path planner with the escoat model and the ru27 trans-atlantic flight data," in *OCEANS 2010 IEEE - Sydney*, pp. 1–10, May 2010.

[8] J. Isern-Gonzalez, D. Hernandez-Sosa, E. Fernandez-Perdomo, J. Cabrera-Gamez, A. Dominguez-Brito, and V. Prieto-Maranon, "Path planning for underwater gliders using iterative optimization," in *Robotics and Automation (ICRA), 2011 IEEE International Conference on*, pp. 1538–1543, may 2011.

[9] R. N. Smith, Y. Chao, P. P. Li, D. A. Caron, B. H. Jones, and G. S. Sukhatme, "Planning and implementing trajectories for autonomous

- underwater vehicles to track evolving ocean processes based on predictions from a regional ocean model,” *International Journal of Robotics Research*, vol. 26, October 2010.
- [10] K. Dahl, D. R. Thompson, D. McLaren, Y. Chao, and S. Chien, “Current-sensitive path planning for an underactuated free-floating ocean sensor-web,” in *International Conference on Intelligent Robots and Systems*, (San Francisco, CA, USA), IEEE/RSJ, 2011.
 - [11] T. Lolla, M. P. Ueckermann, K. Yigit, P. J. Haley, and P. F. J. Lermusiaux, “Path planning in time dependent flow fields using level set methods,” in *ICRA*, pp. 166–173, IEEE, 2012.
 - [12] A. Alvarez, A. Caiti, and R. Onken, “Evolutionary path planning for autonomous underwater vehicles in a variable ocean,” *Oceanic Engineering, IEEE Journal of*, vol. 29, pp. 418 – 429, April 2004.
 - [13] B. Garau, A. Alvarez, and G. Oliver, “Path planning of autonomous underwater vehicles in current fields with complex spatial variability: an A* approach,” in *Robotics and Automation, 2005. ICRA 2005. Proceedings of the 2005 IEEE International Conference on*, pp. 194 – 198, April 2005.
 - [14] D. Kruger, R. Stolkin, A. Blum, and J. Briganti, “Optimal AUV path planning for extended missions in complex, fast-flowing estuarine environments,” in *Robotics and Automation, 2007 IEEE International Conference on*, pp. 4265 –4270, April 2007.
 - [15] J. Witt and M. Dunbabin, “Go with the flow: Optimal AUV path planning in coastal environments autonomous systems,” in *Australasian Conference on Robotics and Automation*, December 2008.
 - [16] T. Inanc, S. C. Shadden, and J. E. Marsden, “Optimal trajectory generation in ocean flows,” in *American Control Conference*, pp. 674–679, 2004.
 - [17] M. Soullignac, “Feasible and optimal path planning in strong current fields,” *Robotics, IEEE Transactions on*, vol. 27, pp. 89 –98, February 2011.
 - [18] R. N. Smith and M. Dunbabin, “Controlled drift: An investigation into the controllability of underwater vehicles with minimal actuation,” in *Proceedings of the Australasian Conference on Robotics and Automation*, 2011, submitted.
 - [19] R. Smith and V. Huynh, “Controlling minimally-actuated vehicles for applications in ocean observation,” in *FAC Workshop on Navigation, Guidance and Control of Underwater Vehicles (NGCUV’2012)*, (University of Porto, Porto, Portugal), pp. 31–36, 2012.
 - [20] R. N. Smith, M. Schwager, S. L. Smith, B. H. Jones, D. Rus, and G. S. Sukhatme, “Persistent ocean monitoring with underwater gliders: Adapting sampling resolution,” *Journal of Field Robotics*, vol. 28, no. 5, pp. 714 – 741, 2011.
 - [21] M. P. A. Singapore, “Singapore port statistics.” http://www.mpa.gov.sg/sites/global_navigation/publications/port_statistics/port_statistics.page.
 - [22] E. Chan, P. Tkalic, K.-H. Gin, and J. Obbard, “The physical oceanography of singapore coastal waters and its implications for oil spills,” in *The Environment in Asia Pacific Harbours* (E. Wolanski, ed.), pp. 393–412, Springer Netherlands, 2006.
 - [23] J. Bellingham, Y. Zhang, J. Kerwin, J. Erikson, B. Hobson, B. Kieft, M. Godin, R. McEwen, T. Hoover, J. Paul, A. Hamilton, J. Franklin, and A. Banka, “Efficient propulsion for the tethys long-range autonomous underwater vehicle,” in *Autonomous Underwater Vehicles (AUV), 2010 IEEE/OES*, pp. 1 –7, September 2010.
 - [24] P. Hart, N. Nilsson, and B. Raphael, “A formal basis for the heuristic determination of minimum cost paths,” *Systems Science and Cybernetics, IEEE Transactions on*, vol. 4, no. 2, pp. 100–107, 1968.
 - [25] T. Koay, Y. Tan, Y. Eng, R. Gao, M. Chitre, J. Chew, N. Chandhavarkar, R. Khan, T. Taher, and J. Koh, “Starfish – a small team of autonomous robotic fish,” *Indian Journal of geo-Marine Science*, vol. 40, pp. 157–167, April 2011.
 - [26] P. Tkalic, M. H. Dao, B. M. Ranjan, S. Palani, H. Xu, C. Cui, and H. K. Choo, “Tropical marine hydrodynamic model forecast.” <http://www.porl.nus.edu.sg/forecast/>.
 - [27] P. Tkalic, W. C. Pang, and P. Sundarambal, “Hydrodynamics and eutrophication modelling for singapore straits,” in *The seventh workshop on ocean models for the APEC Region (WOM-7)*, vol. 5, pp. 1–9, September 2002.
 - [28] W. C. Pang and P. Tkalic, “Modeling tidal and monsoon driven currents in the singapore strait,” *Singapore Maritime Port Journal*, pp. 151–162, 2003.
 - [29] D. M. Ha, D. C. Dung, P. Tkalic, and L. S. Yui, “Ocean hydrodynamics model with tidal forcing derived using an artificial neural network,” in *OCEANS 2006 - Asia Pacific*, pp. 1 –6, May 2006.
 - [30] D. Meldrum, “Recent developments at dunstaffnage: the gps-argos drifter, the smart buoy and the mini drifter,” in *Current Measurement, 1999. Proceedings of the IEEE Sixth Working Conference on*, pp. 75 –81, March 1999.